Compendium of NASA Goddard Space Flight Center's Recent Radiation Effects Test Results

Martha V. O'Bryan[1], Seth S. Roffe[2], Edward P. Wilcox[2], Michael J. Campola[2], Jason M. Osheroff[2], Megan C. Casey[2], Matthew B. Joplin[2], Thomas A. Carstens[2], Jonathan D. Barth[2], Landen D. Ryder[2], Kaitlyn L. Ryder[2], Adia M. Wood[2], Jean-Marie Lauenstein[2], and Peter J. Majewicz[2]

1. Science Systems and Applications, Inc. (SSAI);
2. NASA Goddard Space Flight Center (GSFC)

Abstract: We present results and analysis investigating the effects of radiation on a variety of candidate spacecraft electronics to heavy ion and proton induced single event effects (SEE), proton-induced displacement damage dose (DDD), and total ionizing dose (TID).

Introduction

NASA spacecraft are subjected to a harsh space environment that includes exposure to various types of radiation. The performance of electronic devices in a space radiation environment is often limited by their susceptibility to single-event effects (SEE), total ionizing dose (TID), and displacement damage dose (DDD). Ground-based testing is used to evaluate candidate spacecraft electronics to determine risk to spaceflight applications. Interpreting the results of radiation testing of complex devices is quite difficult. Given the rapidly changing nature of technology, radiation test data are most often application-specific and adequate understanding of the test conditions is critical.

Studies discussed herein were undertaken to establish the application-specific sensitivities of candidate spacecraft and emerging electronic devices to single-event SEE including single-event upset (SEU), single-event latchup (SEL), single-event gate rupture (SEGR), single-event burnout (SEB), single-event transient (SET), TID, enhanced low dose rate sensitivity (ELDRS), and DDD effects. All tests were performed between February 2023 and February 2024.

Summary

We have presented data from recent radiation tests on a variety of devices including several commercial parts. It is the authors' recommendation that this data be used cautiously as many tests were conducted under application- or lot-specific test conditions. We also highly recommend that lot-specific testing be performed on any suspect or commercial device.

See full paper for:

- Test Techniques and Setup
- Acknowledgments
- References

Principal Investigator List

Principal Investigator (PI)	Abbreviation
Megan C. Casey	MCC
Matthew B. Joplin	MBJ
Jean-Marie Lauenstein	JML
Jason M. Osheroff	JMO
Seth Roffe	SR
Kaitlyn L. Ryder	KLR
Landen D. Ryder	LR
Edward (Ted) Wilcox	TW

Acronym List

Acronym	Definition
σ	cross section (cm²/device, unless specified as cm²/bit)
σ_{maxm}	cross section at maximum measured LET (cm²/device, unless specified as cm²/bit)
<	SEE observed at lowest tested LET
>	no SEE observed at highest tested LET
CMOS	Complementary Metal Oxide Semiconductor
DDD	Displacement Damage Dose
DDR3	Double Data Rate 3
DDR4	Double Data Rate 4
DUT	Device Under Test
FPGA	Field Programmable Gate Array
FRIB	Michigan State University's Facility for Rare Isotope Beams
GPU	Graphic Processing Unit
GSFC	Goddard Space Flight Center
LBNL	Lawrence Berkeley National Laboratory
LCD	Liquid-Crystal Display
LDC	Lot Date Code
LED	Light Emitting Diode
LET	Linear Energy Transfer
LET_{th}	Linear Energy Transfer threshold (the maximum LET value at which no effect was observed at an effective fluence of 1x10⁷ particles/cm² – in MeV•cm²/mg
LPDDR	Low Power Double Data Rate
MFTF	mean fluence to failure

Acronym	Definition
MGH FRIB	Massachusetts General Hospital (MGH) Francis H. Burr Proton Therapy, Facility for Rare Isotope Beams (FRIB)
MSU	Michigan State University
NEPP	NASA Electronics Parts and Packaging
NOR	Non-volatile storage technology optimized for random access capabilities
NSRL	Brookhaven National Laboratory's NASA Space Radiation Laboratory
n/a	Not Available
PI	Principal Investigator
REAG	Radiation Effects & Analysis Group
ROIC	Readout-Integrated Circuit
SCA	Sensor Chip Assembly
SEB	Single-Event Burnout
SEE	Single-Event Effect
SEFI	Single-Event Functional Interrupt
SEGR	Single-Event Gate Rupture
SEL	Single-Event Latchup
SET	Single-Event Transient
SEU	Single-Event Upset
SSD	Solid State Drive
TAMU	Texas A&M University
TID	Total Ionizing Dose
UCD	University of California at Davis Crocker Nuclear Laboratory
V_{DS}	Drain-Source Voltage
V_{GS}	Gate-Source Voltage

National Aeronautics and Space Administration

Summary of SEE Test Results

Part Number	Manufacturer	LDC (REAG ID#)	Device Function	Technology	PI	Sample Size	Supply Voltage	Test Env.	Test Facility (Test Date)	Test Results: σ in cm²/device, unless otherwise specified
Memories										
MTFDHBK256TDP-1AT12AIYY	Micron	n/a (23-009)	NVMe Solid State Drive	NAND Flash	TW	7	3.3 V	Proton	MGH (Jan 2024)	Unrecoverable failures observed with 200 MeV protons only under active read-write testing. MFTF: 2.22x10¹⁰/cm². Recoverable failures with power cycling observed with 200 MeV protons. MFTF: 1.56x10⁹/cm²
SDBPTPZ-085G-XI	Western Digital	n/a (23-010)	NVMe Solid State Drive	NAND Flash	TW	7	3.3 V	Proton	MGH (Jan 2024)	Unrecoverable failures (MFTF: 1.43x10¹⁰/cm²) observed with 200 MeV protons only under active read-write testing. Recoverable failures (MFTF: 1.86x10¹⁰/cm²) observed with 200 MeV protons during both reading and writing operations.
MT25QU512ABB	Micron	2YA15 (23-025)	Flash Memory	NOR	TW	5	1.8 - 2.0 V	Heavy Ion	LBNL (Dec 2023)	29.4 < SEL LET_{th} < 45.3 MeVcm²/mg at 55°C; SEL LET_{th} < 29.4 at 82°C; σ_{maxm} 9.09x10⁻⁸cm² at 29.4 MeVcm²/mg, 82°C; SEU LET_{th} < 8.2 MeVcm²/mg; SEU σ 1.8x10⁻¹⁶ cm²/bit at 8.2 MeVcm²/mg
Processing										
ZYNQ XC7Z020-1CLG400C	Xilinx	n/a (20-004)	FPGA and ARM Processor on TUL PYNQ-Z2 Board	CMOS	SR	1	12 V	Protons	MGH (Aug 2023)	Performing math operations increases reliability by the cross section metric when L2 cache is enabled by allowing critical cache to be flushed. L1 cache not large enough to store as much critical information, so disabling L2 cache trivially increases reliability.
SAKURA-I	EdgeCortix	n/a (24-001)	AI Coprocessor (PCIe card)	16 GB LPDDR4	SR	1	12 V	Proton	MGH (Jan 2024)	No destructive SEEs observed at 200 MeV protons with a flux reaching ~ 10⁹ p/cm² s. Data errors were observed in the form of inference mispredictions and changes in the output confidence scores.
Diodes										
STTH208UFY	STMicroelectronics	n/a (22-021)	Diode	Si	MCC	25	800 V	Heavy Ion	MSU FSEE (Apr 2023)	SEB LET_{th} > 50.5 MeVcm²/mg at V_R = 800 V
RS1KFSHMWG	Taiwan Semiconductor	n/a (22-022)	Diode	Si	MCC	25	800 V	Heavy Ion	MSU FSEE (Apr 2023)	SEB LET_{th} > 50.5 MeVcm²/mg at V_R = 800 V
HS1KFS	Taiwan Semiconductor	n/a (22-023)	Diode	Si	MCC	25	800 V	Heavy Ion	MSU FSEE (Apr 2023)	SEB LET_{th} > 50.5 MeVcm²/mg at V_R = 800 V
SFF6661	SSDI	2248 (23-003)	N-Channel Power MOSFET	Si	LR/ JMO	11	0V, -5V, -10V	Heavy Ion	MSU FSEE (Apr 2023)	Tested at LET of 50.5 MeV•cm²/mg; No destructive SEEs observed at 65 V_{DS} & 0 V_{GS}; No destructive SEEs observed at 55 V_{DS} & -5 V_{GS}; 3 (1) pass/(fail) at 70 V_{DS} & 0 V_{GS}; 3 fails at 75 V_{DS} & 0 V_{GS}; 4 fails at 55 V_{DS} & -10 V_{GS}
Miscellaneous										
TLK2711-SP	Texas Instruments	1828A (23-026)	Transceiver	0.25 µm CMOS	MCC	5	2.5 V	Heavy Ion	LBNL (Aug 2023)	SEL LET_{th} > 75.6 MeVcm²/mg @75°C
SN54LVTH574-SP	Texas Instruments	2040A (23-027)	Logic	CMOS	MCC	15	3.3 V	Heavy Ion	LBNL (Aug 2023)	SEL LET_{th} > 75.6 MeVcm²/mg @75°C
SSD1351	Soloman Systech	1431 (22-045)	Organic LED Display Drive	CMOS	LR	2	5 V	Heavy Ion	LBNL (Jun 2023)	SEFI LET_{th} < 1.2 MeV•cm²/mg
HXD8357D	Himax Technologies	2050 (22-047)	LCD Display Driver	CMOS	LR	2	5 V	Heavy Ion	LBNL (Jun 2023)	SEFI LET_{th} < ~16 MeV•cm²/mg. Potential range issues due to packaging constraints.

Summary of TID and DDD Test Results

Part Number	Manufacturer	LDC or Wafer# (REAG ID#)	Device Function	PI	Sample Size	Test Env.	Test Facility (Test Date)	Test Results (Effect, Dose Level/Energy, Results)
Power Device								
2N6284	Microchip	P2132CDWR (23-006)	Power Transistor	KLR	6	Gamma	GSFC (Aug 2023)	No degradation observed up to 59.6 krad(Si)
2N5154	VPT	B2321 (23-022)	Power Transistor	KLR	6	Gamma	GSFC (Dec 2023)	No degradation observed up to 61 krad(Si)
Photonics								
EYP-RWL-0808-00800-4000-BFW09-0000	Toptica-Eagleyard	n/a (23-011)	808-nm Laser Diode	MBJ	2	Proton DDD	UCD (Aug 2023)	No observable degradation up to 63-MeV proton fluence of 5.6E11 p/cm².
EYP-RWL-0808-00800-4000-BFW09-0000	Toptica-Eagleyard	n/a (23-011)	Laser Diode	MBJ	2	Gamma	GSFC (Dec 2023)	No degradation observed up to 80 krad(Si).
IF-HS1	Coherent-Dilas	n/a (23-012)	976-nm Laser Diode	MBJ	2	Proton DDD	UCD (Aug 2023)	No observable degradation up to 63-MeV proton fluence of 5.52E11 p/cm².
IF-HS1	Coherent-Dilas	n/a (23-012)	Laser Diode	MBJ	2	Gamma	GSFC (Dec 2023)	No degradation observed up to 80 krad(Si).
CMDFB1030A	II-VI	n/a (23-013)	1030-nm Laser Diode	MBJ	1	Proton DDD	UCD (Aug 2023)	No observable degradation up to 63-MeV proton fluence of 5.87E11 p/cm².
CMDFB1030A	II-VI	n/a (23-013)	Laser Diode	MBJ	1	Gamma	GSFC (Dec 2023)	No degradation observed up to 80 krad(Si).
EPM605	JDSU/Lumentum	n/a (23-014)	Photodiode	MBJ	2	Proton DDD	UCD (Aug 2023)	Photodiode degradation of dark current at 63-MeV proton fluence<7.5E10 p/cm².
EPM605	JDSU/Lumentum	n/a(23-014)	Photodiode	MBJ	2	Gamma	GSFC (Dec 2023)	No degradation observed up to 80 krad(Si).
C30665GH-LC	Excelitas	n/a (23-015)	Photodiode	MBJ	1	Proton DDD	UCD (Aug 2023)	Photodiode degradation of dark current and responsivity at 63-MeV proton fluence<7.5E10 p/cm².
C30665GH-LC	Excelitas	n/a(23-015)	Photodiode	MBJ	1	Gamma	GSFC (Dec 2023)	No degradation observed up to 80 krad(Si).
J22-5IR03M-1.7	Teledyne	n/a (23-016)	Photodiode	MBJ	1	Proton DDD	UCD (Aug 2023)	Photodiode degradation of dark current at 63-MeV proton fluence<7.5E10 p/cm².
J22-5IR03M-1.7	Teledyne	n/a(23-016)	Photodiode	MBJ	1	Gamma	GSFC (Dec 2023)	No degradation observed up to 80 krad(Si).
GAP3000	GPD	n/a (23-017)	Photodiode	MBJ	1	Proton DDD	UCD (Aug 2023)	Photodiode degradation of dark current at 63-MeV proton fluence <7.5E10 p/cm².
GAP3000	GPD	n/a (23-017)	Photodiode	MBJ	1	Gamma	GSFC (Dec 2023)	No degradation observed up to 80 krad(Si).
C30665GH	Excelitas	n/a (24-004)	Photodiode	MBJ	2	Proton DDD	UDC (Feb 2024)	Photodiode degradation of dark current at 63-MeV proton fluence<8.89E11 p/cm².
NIR-MPZ-LN-20	iXblue	n/a (23-018)	Optical Phase Modulator	MBJ	1	Proton DDD	UCD (Aug 2023)	No observable degradation up to a 63-MeV proton fluence of 5.89E11 p/cm².
NIR-MPZ-LN-20	iXblue	n/a (23-018)	Optical Phase Modulator	MBJ	1	Gamma	GSFC (Dec 2023)	No degradation observed up to 80 krad(Si).
BBM2-NIR-MPX-LN-01	iXblue	n/a (23-019)	Optical Phase Modulator	MBJ	1	Proton DDD	UCD (Aug 2023)	No observable degradation up to a 63-MeV proton fluence of 5.89E11 p/cm².
BBM2-NIR-MPX-LN-01	iXblue	n/a (23-019)	Optical Phase Modulator	MBJ	1	Gamma	GSFC (Dec 2023)	No degradation observed up to 80 krad(Si).
SCD-T80156 rev A	DiCon	n/a (24-005)	Optical Switch	MBJ	2	Proton DDD	UCD (Feb 2024)	No observable degradation up to a 63-MeV proton fluence of 8.95E10 p/cm².
113-00148	Coherent Electro-Optics Technology	n/a (24-006)	High Power Isolator	MBJ	2	Proton DDD	UCD (Feb 2024)	No observable degradation up to a 63-MeV proton fluence of 8.95E10 p/cm².
OD-110L	Opti Diode	n/a (23-028)	GaAlAs 850 nm LED	JML	4	Proton DDD	UCD (Aug 2023)	Step irradiation to up to 63 MeV proton fluence of 3.40x10¹²/cm² (451 krad(Si)). Relative optical intensity decreased between 47.1% - 48.5% at the maximum dose; no spectral shift or widening of the output spectrum. [19]
NC4U334BR	Nichia	n/a (23-029)	AlGaN 280 nm LED	JML	2	Proton DDD	UCD (Aug 2023)	Step irradiation to up to 63 MeV proton fluence of 3.43x10¹²/cm² (456 krad(Si)). Relative optical intensity decreased ≤ 10% at max dose; no spectral shift or widening of output spectrum.
NCSU434C	Nichia	n/a (23-030)	AlGaN 280 nm LED	JML	2	Proton DDD	UCD (Aug 2023)	Step irradiation to up to 63 MeV proton fluence of 3.43x10¹²/cm² (456 krad(Si)). Relative optical intensity decreased ≤ 10% at max dose; no spectral shift or widening of output spectrum.
XFM-5050-UV	Luminus	n/a (23-031)	AlGaN 280 nm LED	JML	2	Proton DDD	UCD (Aug 2023)	Step irradiation to up to 63 MeV proton fluence of 3.43x10¹²/cm² (456 krad(Si)). Relative optical intensity decreased ≤ 10% at max dose; no spectral shift or widening of output spectrum.
Thermistors								
QT06020-142	Qti	n/a (23-020)	Thermistor	MBJ	2	Gamma	GSFC (Dec 2023)	No degradation observed up to 80 krad(Si).
QT06020-142	Qti	n/a (23-020)	Thermistor	MBJ	2	Proton DDD	UCD (Aug 2023)	Thermistor showed variation in temperature linearity between 63-MeV-proton 7.5e10 p/cm² and 1.5e11 p/cm² fluence.

Micron MTFDHBK256TDP-1AT12AIYY SSD

Six devices were tested at the Francis H. Burr Proton Therapy Center at Massachusetts General Hospital.

To maintain realistic operating conditions, the devices were tested with 1 GB of pseudorandom data written and read from random locations (changing each cycle) through the SSD memory space. Each write/read loop takes about 10 seconds to complete at this scale. Operations were performed from a Windows 10-based computer using Python test code that used the wmic module to perform low level (raw) block operations.

DUT mounted to passive PCIe extender for testing.

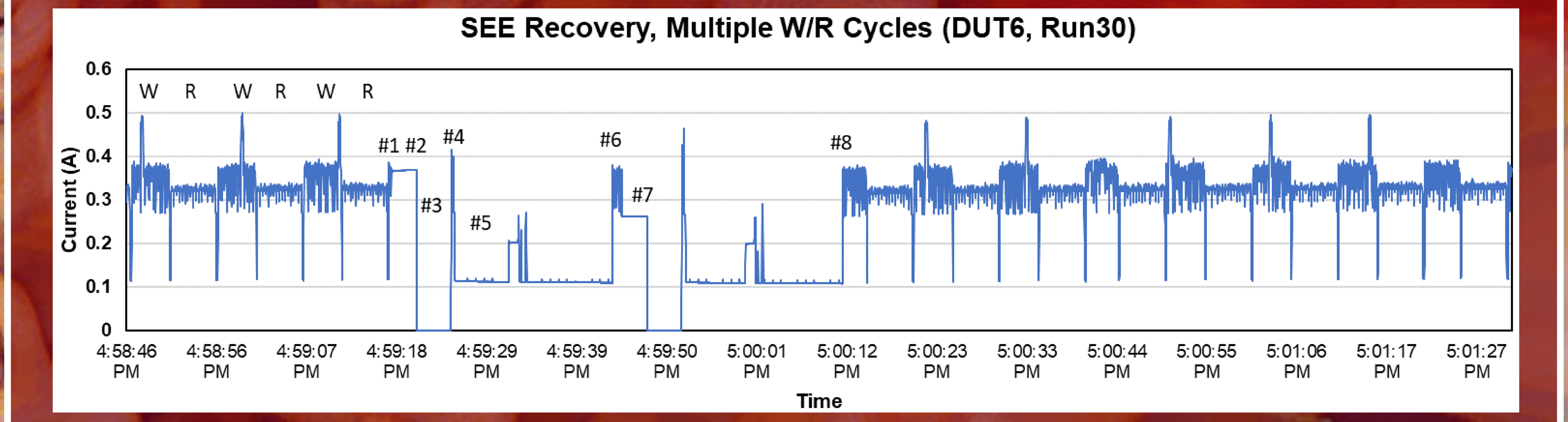

Two SEFI observed and recovered in quick succession during 200 MeV proton testing.

The sequence below describes the subsequent events, marked with numbers on the chart above.

1. Initiation of a write command at 4:59:17 PM. The supply current elevates but is uncharacteristically flat.
2. Three seconds later at 4:59:20 PM the test software throws an exception when the write has failed to complete. This is classified as a timeout error.
3. The power supply is disabled for four seconds and the proton beam is inhibited.
4. At 4:59:24 PM power is restored
5. The device is allowed 20 seconds to initialize, still without beam applied.
6. At 4:59:44 PM the beam is uninhibited and testing (the incomplete write) resumes
7. Writing proceeds successfully for about 2 seconds until it again hangs for 3 seconds, triggering a timeout error and a repeat of the recovery in steps 3-6).
8. Writing resumes after the second recovery and completes. The subsequent read operation is successful, along with the depicted write and read cycles afterwards.

Fluence Between Failure with Proton Irradiations

Device #	Total Failure Events	Total Biased Fluence	Mean Fluence Between Failure	Tested until unrecoverable error occurred?
Micron_2	2	4.28E+09	2.14E+09	Yes
Micron_3	7	6.97E+09	9.96E+08	Yes
Micron_4	4	8.82E+09	2.21E+09	Yes
Micron_5	14	1.46E+10	1.04E+09	Yes
Micron_6	13	2.06E+10	1.58E+09	No
Micron_7	9	2.38E+10	1.98E+09	No
Micron_8	9	1.26E+10	9.42E+08	No
sum	*58*	*9E+10*	*1.56E+09*	

Xilinx Zynq-7020 SoC on the TUL PYNQ-Z2 board

The results of the tests were separated into configurations where the L2 cache was on and off, shown in Figures below. When the L2 cache is ON, the MFTF is significantly worse for the IDLE configurations compared to the MM configurations. This is most likely due to the critical data retrieval processes of the DUT. When matrix multiplication is processing, critical kernel data is being flushed out of the cache to make room for the matrix data. If the system is idling, then that critical data never gets flushed out of the cache and thus has a higher chance of corruption, especially since the DDR3 SDRAM chip was not under irradiation. Additionally, the UNLOADED configurations were significantly better than the LOADED configurations. This implies that the drivers being loaded and active in the kernel do affect the reliability of the system. This is expected since the drivers have memory access to kernel space, even when they aren't actively being used. However, the number of drivers installed and loaded do not seem to have a significant effect on cross section.

We surmise that this could be because there wasn't enough of a significant difference in the number of drivers between the configurations, or because the drivers were not being actively used on real hardware devices. In the L2 cache OFF configuration, any patterns are much more difficult to discern, most likely due to there being not enough memory space in the L1 cache to hold critical data.

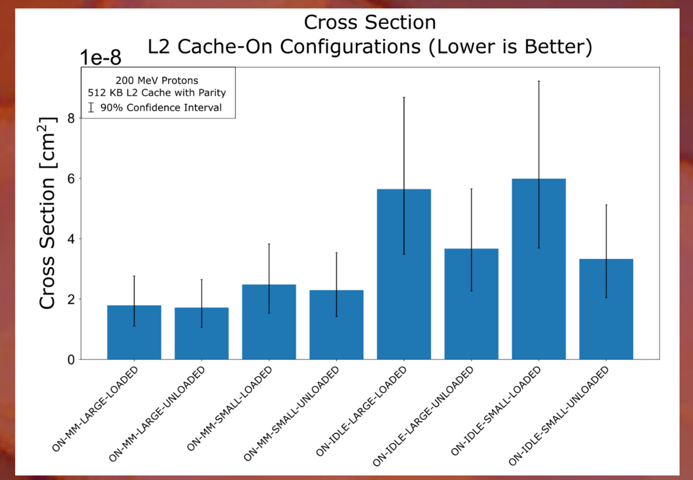

Results with L2 Cache On.

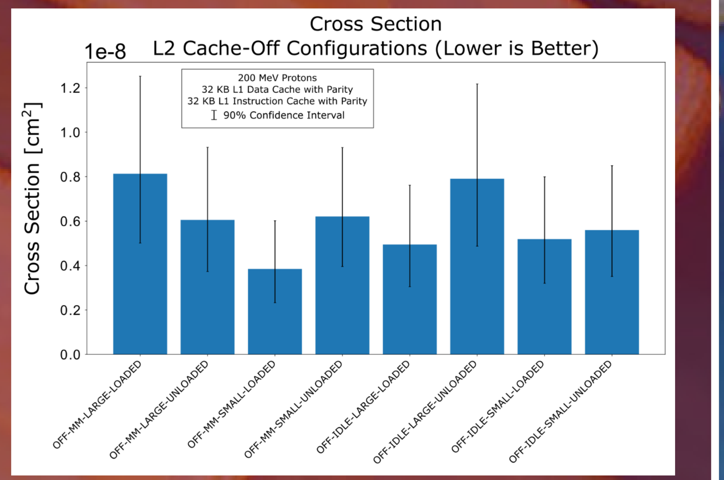

Results with L2 Cache Off.